CCS Chemistry

COMMUNICATION

Received: Aug. 30, 2020 | Accepted: Nov. 18, 2020

Improving Water Stability of Metal–Organic Frameworks by a General Surface Hydrophobic Polymerization

Meili Ding[1,2] & Hai-Long Jiang[1]*

[1]*Hefei National Laboratory for Physical Sciences at the Microscale, CAS Key Laboratory of Soft Matter Chemistry, Department of Chemistry, University of Science and Technology of China, Hefei, Anhui 230026,* [2]*College of Chemical Engineering, Nanjing Forestry University, Nanjing, Jiangsu 210037*

**Corresponding author: jianglab@ustc.edu.cn*

Cite this: *CCS Chem.* **2020**, *2*, 2740–2748

Water and moisture stability have been recognized as one of the most important characteristics of metal–organic frameworks (MOFs) in regards to their future applications. Nonetheless, most MOFs are water-labile to some degree. One promising solution for the collapse of MOFs toward water is surface hydrophobic modification. Herein, a facile, mild, and general one-step surface polymerization approach has been developed to coat the exterior surface of MOF particles with a thin polymer layer. Remarkably, the hydrophobic layer not only endows water stability of MOFs without significantly disturbing their pore features but also enables the resultant MOFs to retain high catalytic performance for diverse reactions in water.

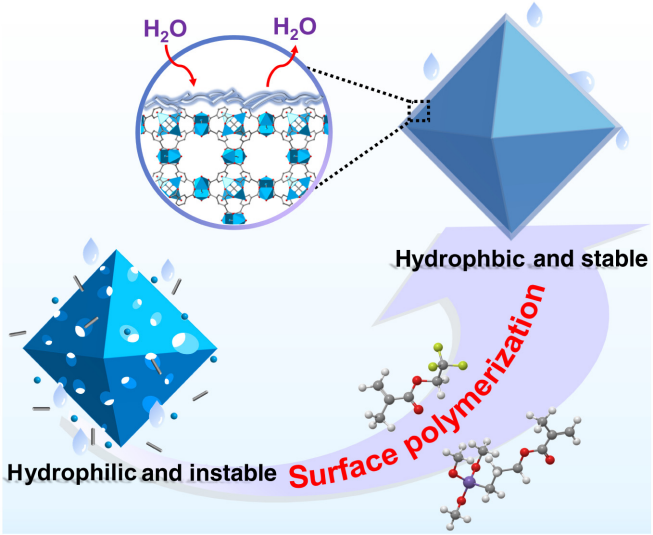

Keywords: water stability, metal–organic frameworks, hydrophobic, polymerization, composite

Introduction

Emerging as an important class of porous materials, metal–organic frameworks (MOFs), have received tremendous scientific attention in the last two decades.[1–4] The well-defined and highly tunable structures as well as the high surface areas make MOFs great options for diverse applications, especially in heterogeneous catalysis.[5–24] However, water stability remains a grand challenge in the real-world application of most MOFs.[25–27] A significant fraction of MOFs are vulnerable to structural destruction in an aqueous environment because of the gradual replacement of metal-coordinated linkers by water molecules.[25–27] It should be noted that moisture or water stability is regarded as the most basic feature of MOFs for subsequent applications.

Careful selection of MOF constituents is a feasible approach to fabricate water-stable MOFs via de novo synthesis.[25,26,28–33] However, the synthesis of MOFs is generally difficult to control, and the resultant MOF

DOI: 10.31635/ccschem.020.202000515
CCS Chem. **2020**, *2*, 2740–2748

structures are hardly predictable. Although the high-connectivity MOFs, which are built from multicarboxylate linkers, tend to exhibit excellent chemical and thermal stability, the presynthesis of these linkers is usually complicated, increasing the production cost of the resultant MOFs. In addition, the introduction of dangling hydrophobic groups, such as various alkyl groups, can protect the frameworks against decomposition; however, this usually significantly decreases surface area and porosity, thereby causing a mass transfer issue throughout of MOF.[34–37]

Not limited to de novo synthesis, given the desirable attributes of many reported MOFs, the exploration of postsynthetic strategies has gained significant momentum over the past few years.[26,31,32] Various postsynthetic approaches have been adopted to improve the water stability of MOFs: functional group modification, ion-exchange, hydrophobic surface treatment, and material compositization.[38–51] The surface wettability or the reactivity of metal clusters can be regulated using these methods, thereby improving the water stability of MOFs. Unfortunately, the current postsynthetic approaches involve realistic challenges and prerequisites: (1) uneven coating of the protective layer on MOFs, (2) specific active groups on the MOF skeleton for postsynthetic modifications, and (3) pore space occupancy in MOFs after modification.[26,31,32] In this context, our group developed a general approach to coat hydrophobic polydimethysiloxane (PDMS) on the external surface of MOFs.[38] The coated MOFs, with protection from the PDMS layer, present remarkably improved moisture and water stability in comparison to the parent MOFs. Nevertheless, the coating process must be completed at a high operation temperature (235 °C), and it is difficult to achieve uniform coating on the surface of overall MOF particles by the vapor deposition technique. The Martí-Gastaldo group[50] reported a facile strategy to produce catechol coatings on the external surface of Hong Kong University of Science and Technology-1, based on the Cu(II) dimer-catalyzing polymerization of catechols, improving the Cu–MOF water stability. This approach is effective for Cu–MOFs, yet it might not be applicable to other types of MOFs. Recently, the Li group[51] successfully fabricated a series of MOF@polymer via surface-initiated atom transfer radical polymerization (SI-ATRP). The random copolymer temporarily immobilized on MOF surfaces can serve as macroinitiator to initiate SI-ATRP. Significantly, the polystyrene shell effectively protects the UiO-66 MOF from the attack of acid and base. Unfortunately, N_2 uptake dramatically decreases in the coated MOFs due to the low mobility of polymer layers. Therefore, there remains a need to explore a facile, mild, efficient, and universal approach to improve the moisture stability of MOFs without significantly compromising their pore features. Moreover, the increased moisture stability might enable the active yet moisture-sensitive MOFs for catalytic applications in water.

Herein, we demonstrate a postsynthetic modification strategy, namely one-step surface polymerization, which we propose as an effective way to improve the moisture stability of MOFs and further manipulate MOFs' catalytic properties. Taking HKUST-1 as a representative, a hydrophobic polymer layer can be formed on the HKUST-1 surface through the radical copolymerization of two monomers—2,2,2-trifluoroethyl methacrylate (TFEMA) and 3-methacryloxypropyltrimethoxysilane (MAPTMS)—giving a hydrophobic composite, denoted HKUST-1-P (Scheme 1). Because of the protection from the hydrophobic polymer overlayer, the crystalline nature and morphology of HKUST-1 can be maintained even after exposure to water for 3 days. Notably, the pore characteristics of HKUST-1 remain essentially unchanged, as the

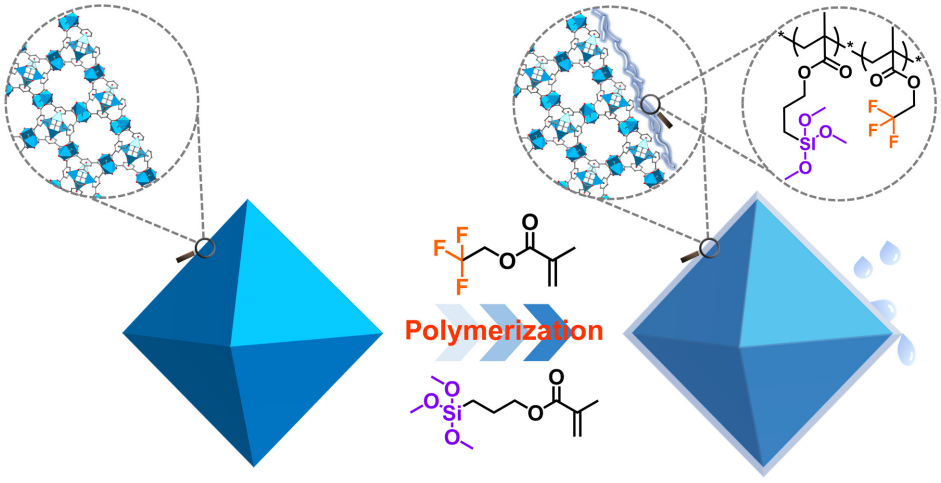

Scheme 1 | *Schematic illustration showing the one-step surface polymerization of HKUST-1 to afford hydrophobic HKUST-1-P composite.*

DOI: 10.31635/ccschem.020.202000515
CCS Chem. **2020**, *2*, 2740–2748

polymer layer is mainly located on the MOF surface. To prove the versatility of this approach, two other water-sensitive MOFs, ZIF-67 and MIL-125, were readily coated with this hydrophobic polymer based on a similar approach. Additionally, we were delighted to find that HKUST-1-P exhibits superior catalytic conversion and cycling stability for organic synthesis in water in comparison with the originally water-sensitive HKUST-1 because of the protective effect and the hydrophobicity endowed by the polymer overlayer.

Results and Discussion

The HKUST-1, formulated $Cu_3(BTC)_2{\cdot}3H_2O$ (BTC = 1,3,5-benzene tricarboxylate), is one of the most studied MOFs because of its low cost, easy preparation, high surface area, and tremendous potential in gas adsorption, heterogeneous catalysis, and so on.[52,53] Unfortunately, prolonged exposure to a humid operating environment gives rise to severe structural damages in HKUST-1 due to the hydrolysis of the Cu–O bonds involved in the paddle-wheel building blocks. With the above considerations, HKUST-1 was chosen as the representative sample. Typically, the coating process is performed by dispersing the two monomers, TFEMA and MAPTMS, into the ethanol solution of HKUST-1. Then the polymerization process is initiated by introducing 2,2′-azobis(isobutyronitrile) (AIBN) at a moderate temperature (75 °C) under a nitrogen (N_2) atmosphere (see "Experimental Section" in Supporting Information). Specifically, the monomers are first linked on the external surface of HKUST-1 because of the hydrogen bonds between the carbonyl oxygen atoms in the two kinds of monomers and the coordinated water molecules in HKUST-1,[54] and then the copolymerization is carried out in the presence of AIBN (see Supporting Information Figure S1a). The polymerization process consists of the following two steps (see Supporting Information Figure S1b): the dissociation of AIBN to form radical species and the addition of one monomer to the aforementioned initiating radical (initiation), and the subsequent increase of chain length through the addition of other monomers (chain propagation).[55,56] Undoubtedly, the thickness of the coating layer can be easily tuned by changing the reaction time or the concentration of monomers or AIBN. The quantitation of polymer overlayer in composites by thermogravimetric analysis (TGA) is not feasible due to the weight losses at similar temperature ranges for the polymer overlayer and HKUST-1 (see Supporting Information Figure S2). Given the periodic structures of MOFs, inductively coupled plasma atomic emission spectroscopy (ICP-AES) was carried out to quantify the total copper content, thereby elucidating the MOF weight percentage. Accordingly, the content of the polymer overlayer within HKUST-1-P composite was ~8.27 wt% (see Supporting Information Table S1).

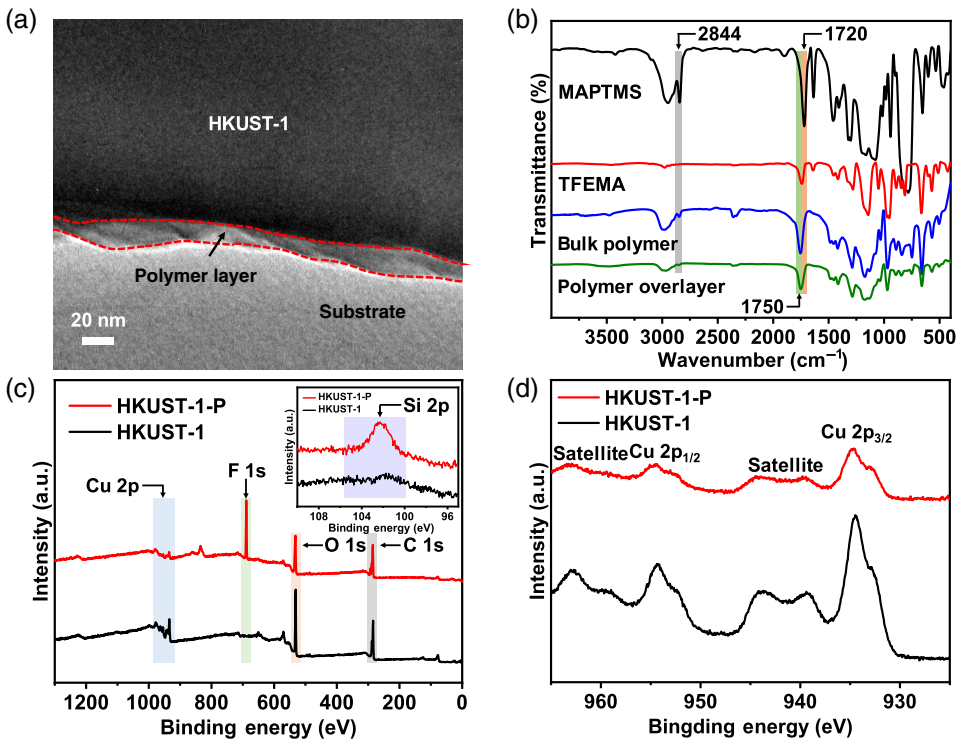

Figure 1 | *(a) TEM image of HKUST-1-P sample, highlighting the polymer edge. (b) FT-IR spectra of MAPTMS, TFEMA, bulk polymer, and polymer overlayer. (c) XPS survey spectra for HKUST-1 and HKUST-1-P. (d) High-resolution XPS spectra of Cu 2p for HKUST-1 and HKUST-1-P.*

DOI: 10.31635/ccschem.020.202000515
CCS Chem. **2020**, *2*, 2740–2748

The transmission electron microscopy (TEM) image clearly shows a layer of ~14 nm thickness on the external surface of the HKUST-1-P particle (Figure 1a), confirming the location of polymer in the composite. To our delight, the degree of polymerization or rate of polymerization can be tuned, to some extent, by changing the reaction time or the concentration of monomers or AIBN, eventually influencing the thickness of the coating overlayer.[57] For instance, the layer thickness increases to ~85, 37, and 70 nm with increased polymerization time, amount of initiator, and concentration of two monomers, respectively (see Supporting Information Figure S3). The increased polymer content was also indicated by the weight percentage of polymer overlayer within these three samples, as calculated based on ICP-AES results (see Supporting Information Table S2).

The successful polymerization of two monomers was demonstrated by Fourier transform infrared (FT-IR) spectroscopy (Figure 1b). For comparison, bulk polymer was prepared under the same reaction conditions in the absence of MOFs, and the polymer overlayer of HKUST-1-P was peeled off from the composite through acid treatment. To our delight, the two polymers displayed almost the same IR spectra. The occurrence of the band at 2844 cm^{-1} in bulk polymer and polymer overlayer correlates with the CH_3 symmetric stretch in the Si–O–CH_3 groups of MAPTMS.[58] The intense adsorption band at 1750 cm^{-1} of both polymer materials can be assigned to the C=O stretching of TFEMA, whereas the peak at 1720 cm^{-1} in MAPTMS is due to the ester C=O stretching vibration of the carbonyl group.[59,60] Altogether, these results indicate that the polymer overlayer of HKUST-1-P is composed of the two monomers.

X-ray photoelectron spectroscopy (XPS) spectra suggest the presence of C, O, and Cu in HKUST-1, and C, O, Si, F, and Cu in HKUST-1-P (Figure 1c). The relatively reduced signal of the Cu 2p peak is observed in the spectrum of HKUST-1-P when compared with that of HKUST-1 (Figure 1d), further proving the location of the polymer. Additionally, the almost identical Cu 2p peak positions of Cu $2p_{1/2}$ and $2p_{3/2}$ in both samples suggest that the integration of HKUST-1 and the polymer layer may not rely on the coordination interaction between polymer and the Cu atoms of HKUST-1.

The wettability of HKUST-1 and HKUST-1-P was evaluated by the measurement of the static contact angle. The contact angle of a water droplet on HKUST-1 was ~0°, demonstrating its hydrophilic property (Figure 2a). In stark contrast, upon polymer coating, HKUST-1-P exhibits water contact angle ~135° (Figure 2b). The distinct surface character, from hydrophilic to hydrophobic, can be attributed to the introduction of the polymer overlayer. It has been well documented that surface hydrophobicity would increase the water stability of MOFs.[26,31,33–37] To examine the water stability of HKUST-1-P, both parent and modified MOF samples were exposed to water for 3 days. HKUST-1 can easily settle down to the bottom of the water owing to its good hydrophilicity (Figure 2c). Accordingly, the flocculent precipitate can be observed around the MOF particles at the bottom of the bottle over time (Figure 2d). Because of the low density and hydrophobic behavior, HKUST-1-P mostly floated on the water during the 3-day hydrostability test (Figures 2e and 2f). The powder X-ray diffraction (XRD) pattern of HKUST-1-P shows sharp characteristic peaks indexed to HKUST-1 (Figure 2g), demonstrating the crystallinity retention of HKUST-1 after coating the polymer layer. More importantly, upon the same water treatment, significant loss of structural integrity was observed for HKUST-1, while the crystallinity of HKUST-1-P remained essentially unchanged, manifesting the greatly enhanced framework stability against degradation from water.

To investigate the impact of surface wettability on the microstructure, the morphology of HKUST-1 and HKUST-1-P was examined using scanning electron microscopy (SEM). The pristine HKUST-1 had an octahedral

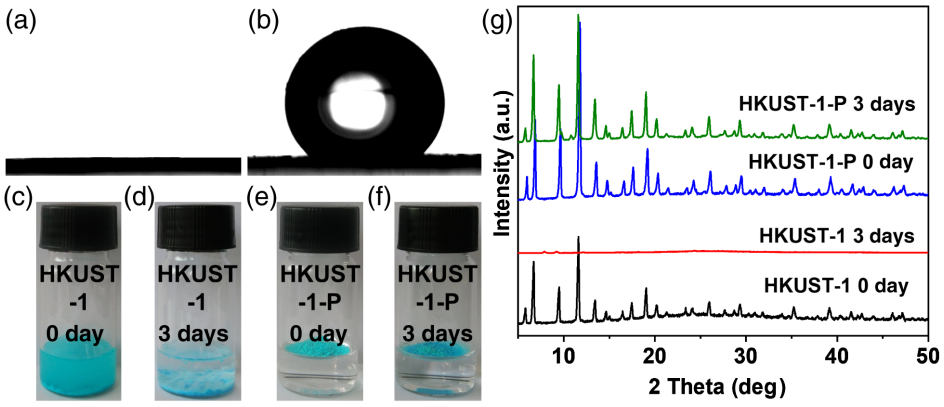

Figure 2 | *Static contact angles of water on (a) HKUST-1 and (b) HKUST-1-P. (c–f) Digital photographs and (g) powder XRD profiles of HKUST-1 and HKUST-1-P before and after 3 days of hydrostability test.*

DOI: 10.31635/ccschem.020.202000515
CCS Chem. **2020**, *2*, 2740–2748

morphology and a smooth surface (Figure 3a). After water treatment for 3 days, the octahedral morphology nearly disappeared (Figure 3b). In contrast to HKUST-1, the octahedral morphology of HKUST-1-P particles was well preserved after immersion in water for the same duration (Figures 3c and 3d). The porosity of the two samples was evaluated via N_2 adsorption measurements at 77 K (Figure 3e). As expected, the N_2 isotherms suggest that the Brunauer–Emmett–Teller (BET) surface area of HKUST-1 significantly dropped by ~100% from 1451 to 0.5 m^2/g upon immersion in water for 3 days, demonstrating a complete framework collapse. It is worth noting that the BET surface area of HKUST-1-P was as high as 1352 m^2/g, and no evident change was observed in the pore size distribution after coating with the polymer layers (see Supporting Information Figure S4). The results suggest that the pore features of HKUST-1 remain essentially unchanged, and the polymerization of two monomers is mostly completed to afford a polymer overlayer on the external surface of HKUST-1. To our delight, HKUST-1-P displayed only a minor decrease (~2%) in BET surface area after the same exposure to water, which is perfectly consistent with the XRD and SEM results.

In addition to enhanced water stability at room temperature, we were delighted to find that the polymer overlayer provides a protective barrier impeding the ingression of water at even a higher operation temperature. Specifically, HKUST-1-P displays outstanding tolerance after exposure to water at 50 °C, in sharp contrast to the pristine HKUST-1 (see Supporting Information Figures S5–S7). The phase transformation of HKUST-1 after water treatment is consistent with that reported in the literature.[61] To further demonstrate the stability of the polymer overlayer, the structural integrity of HKUST-1-P was investigated in various organic solvents. The results showed that there was no significant change in the morphology, crystallinity, and porosity of HKUST-1-P after being soaked in organic solvents (*N*,*N*-dimethyl formamide, methanol, and ethanol) for 24 h (see Supporting Information Figures S8–S10), suggesting a high structural stability of the coating polymer.

To verify the necessity of MAPTMS, HKUST-1 coated with homopolymers (denoted as HKUST-1-HP) was prepared as a control under similar conditions in the absence of MAPTMS. Unexpectedly, upon the same 3-day water treatment, the surface area of HKUST-1-HP was dramatically reduced from 1279 to 61 m^2/g (see Supporting Information Figure S11). In addition, extreme erosion was found in the morphology of HKUST-1-HP, and obvious phase change was also recorded by powder XRD analysis (see Supporting Information Figures S12 and S13). The results clearly illustrate the particular role of MAPTMS in the formation of water-stable HKUST-1-P.

To demonstrate the universality of this overlayer coating strategy, two other representative MOFs, ZIF-67 and MIL-125,[62,63] which have completely different metals, linkers, and structures from HKUST-1, were coated with the hydrophobic polymer in the same way. As expected, the water contact angles of ZIF-67 and MIL-125 increased from 0° to 146° and 141°, respectively, after integrating with the hydrophobic polymer (see Supporting Information Figure S14). Furthermore, all the XRD, SEM, and N_2 adsorption and desorption data clearly suggest that the coated ZIF-67 (ZIF-67-P) exhibits superior water stability as compared to the parent ZIF-67 upon the same water treatment for 4 days (see Supporting Information Figures S15–S17). In contrast with the parent MIL-125, MIL-125-P maintained its crystallinity, morphology, and porosity after a 5-day exposure to water (see Supporting Information Figures S18–S20). All these results strongly demonstrate that this postsynthetic approach does not require any special active groups to integrate the

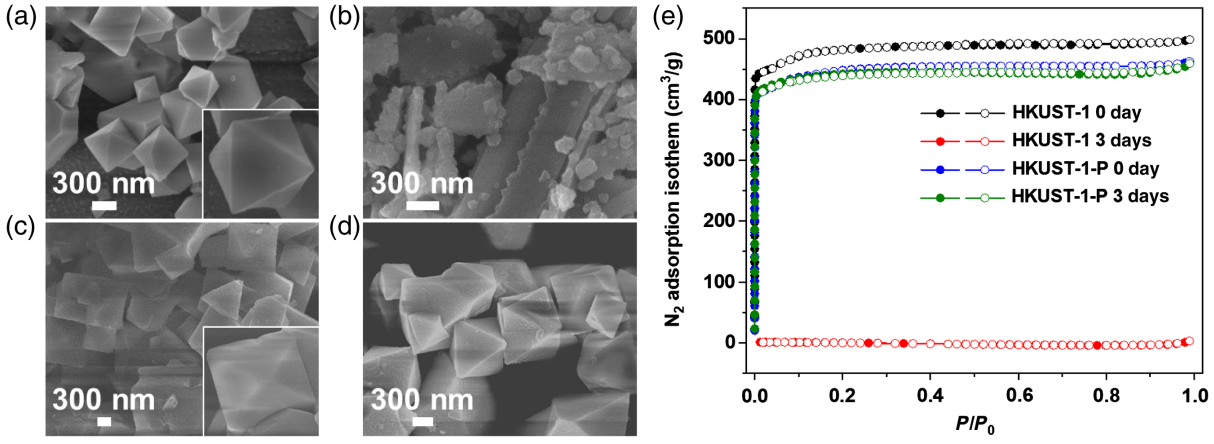

Figure 3 | *SEM images of (a and b) HKUST-1 and (c and d) HKUST-1-P (left) before and (right) after exposure to water for 3 days (inset: enlarged images). (e) N_2 sorption isotherms for HKUST-1 and HKUST-1-P before and after exposure to water for 3 days.*

DOI: 10.31635/ccschem.020.202000515
CCS Chem. **2020**, *2*, 2740–2748

water-labile MOFs with polymer overlayer, highlighting the generality of this strategy. Moreover, the increased hydrophobicity arising from the polymer overlayer can effectively reduce the exposure of metal clusters to water, endowing the resultant MOFs with high tolerance to humid environments.

We envision that the enhanced water stability and surface hydrophobicity will make the resultant MOF composites ideal heterogeneous catalysts for reactions in water. It is widely recognized that water is a green, sustainable, and promising solvent in catalytic syntheses on account of its nontoxicity, abundance, and renewability.[64,65] The synthesis of benzimidazole, a classical Lewis-acid catalyzed reaction, was initially chosen for investigation due to its great potential in the development of pharmacologically active compounds.[66] Along this line, the reaction is initiated by adding benzaldehyde and the aqueous solution of *o*-phenylenediamine to a round-bottom flask containing activated HKUST-1 or HKUST-1-P under magnetic stirring at 25 °C. As expected, HKUST-1-P possesses remarkable catalytic activity with a high yield of >99% (Figure 4a). Under the same reaction conditions, nearly 94% yield was achieved for HKUST-1. To further clarify the effect of water stability and surface hydrophobicity on the catalytic performance of MOFs, the same reaction procedure was conducted three times with HKUST-1 and HKUST-1-P, respectively. Impressively, the catalytic activity of HKUST-1-P was maintained during the three successive reactions. In contrast, the yield of benzimidazole gradually decreased to 63% in the third run over HKUST-1. Surprisingly, the powder XRD patterns of both HKUST-1 and HKUST-1-P after three recycling experiments showed almost retained crystallinity (see Supporting Information Figure S21).

To understand the reason behind the different recycling performance between HKUST-1 and HKUST-1-P, SEM observation and N_2 adsorption/desorption studies of these two catalysts after three catalytic cycles were performed (see Supporting Information Figures S22 and S23). Serious particle corrosion was found in HKUST-1, whereas the original morphology of HKUST-1-P remained intact, explaining the excellent recycling stability and performance of the latter in the synthesis of benzimidazole. Furthermore, the BET surface area of HKUST-1 dramatically reduced (from 1451 to 135 m^2/g), while HKUST-1-P shows a minor change (from 1352 to 1017 m^2/g) only, after the three runs of catalytic reaction. This also demonstrates the decent stability of the hydrophobic HKUST-1-P composite. The difference between the crystallinity and surface area of HKUST-1 after catalytic cycling can be attributed to the different functions of powder XRD and N_2 adsorption measurements. Generally, the results obtained by N_2 adsorption measurement are more convincing and sensitive to evaluate the porous structures of MOFs.[67] The combination of multiple detection analysis methods is more reliable to confirm the structural integrity of MOFs. In addition, the above results unambiguously prove that external hydrophobic treatment does not block substrates from accessing the catalytically active sites, and the hydrophobic polymer overlayer plays a critical role in the catalytic reactions in

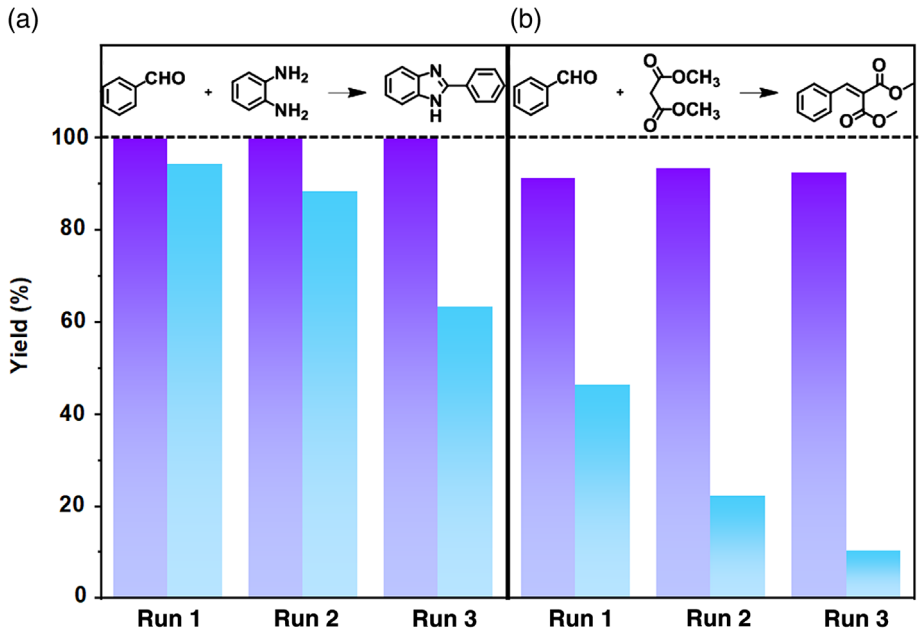

Figure 4 | *Recycling performance comparison between HKUST-1-P (purple) and HKUST-1 (blue) in the three consecutive catalytic runs in (a) the synthesis of benzimidazole and (b) the Knoevenagel condensation reaction.*

DOI: 10.31635/ccschem.020.202000515
CCS Chem. **2020**, *2*, 2740–2748

water, particularly with originally moisture-sensitive MOFs.

Encouraged by the significantly improved catalytic properties of HKUST-1-P with respect to its parent MOF, we sought to investigate their catalytic performance in the Knoevenagel condensation reaction with benzaldehyde and dimethyl malonate. Knoevenagel condensation, which is a general route to C–C bond formation, can be catalyzed with Lewis basic or acidic sites.[10] Using water as the solvent, HKUST-1-P achieved a good yield of 91% after being stirred at 60 °C for 12 h (Figure 4b). Nevertheless, only 46% conversion of substrate into the target product over HKUST-1 was observed under identical conditions. Such a huge difference in catalytic activity between these two catalysts can be attributed to the much higher surface hydrophobicity of HKUST-1-P in comparison with HKUST-1. This feature might allow hydrophobic substrates such as dimethyl malonate to be enriched around the active sites in HKUST-1-P. In addition, HKUST-1-P exhibits excellent recycling performance without an activity drop in three consecutive cycles; by contrast, the yield sharply decreases to 10% with HKUST-1 in the third run. Like the previous reaction, no significant loss of crystallinity for HKUST-1 and HKUST-1-P was observed based on the powder XRD patterns (see Supporting Information Figure S24). The SEM images demonstrate that HKUST-1 underwent serious corrosion in the reaction, whereas HKUST-1-P particles essentially preserve their original morphology due to the protection endowed by the hydrophobic polymer overlayer (see Supporting Information Figure S25). Similar observations were made with N_2 adsorption/desorption isotherms for these two catalysts (see Supporting Information Figure S26). Upon recycling experiments, a significant drop in N_2 uptake capacity revealed the structural change of HKUST-1, while the slightly decreased surface area of HKUST-1-P might be ascribed to the partial occupation of the pore space by the residual product. All the results clearly suggest that the water stability and surface hydrophobicity created by surface polymerization strategy make HKUST-1-P an efficient and stable Lewis acid catalyst for organic reactions in an aqueous environment.

Conclusion

We have developed a facile and universal approach to coating a thin hydrophobic polymer overlayer on MOF surfaces via one-step surface polymerization. Remarkably, the external hydrophobic overlayer serves as a shield to protect the weak metal–ligand bond from attack of water molecules. More importantly, thanks to the high water stability and hydrophobicity endowed by the polymer overlayer, the resultant MOFs exhibit excellent catalytic activity and recyclability toward water-mediated organic reactions, far surpassing the parent MOFs. This work not only provides a facile and general protocol to improve water or moisture stability of MOFs but also paves the way for the targeted fabrication of MOF-based composites by the rational integration of their specific attributes for diverse applications.

Supporting Information

Supporting Information is available and includes detailed experimental procedures and additional figures.

Conflict of Interest

There is no conflict of interest to report.

Acknowledgments

The authors acknowledge financial support by the National Natural Science Foundation of China (nos. 21725101, 21673213, 21871244, and 21521001).

References

1. Furukawa, H.; Cordova, K. E.; O'Keeffe, M.; Yaghi, O. M. The Chemistry and Applications of Metal-Organic Frameworks. *Science* **2013**, *341*, 1230444.
2. Zhou, H.-C.; Kitagawa, S. Metal-Organic Frameworks (MOFs). *Chem. Soc. Rev.* **2014**, *43*, 5415–5418.
3. Li, B.; Wen, H.-M.; Cui, Y.; Zhou, W.; Qian, G.; Chen, B. Emerging Multifunctional Metal-Organic Framework Materials. *Adv. Mater.* **2016**, *28*, 8819–8860.
4. Wang, H.; Zhu, Q.-L.; Zou, R.; Xu, Q. Metal-Organic Frameworks for Energy Applications. *Chem* **2017**, *2*, 52–80.
5. Jiao, L.; Seow, J. Y. R.; Skinner, W. S.; Wang, Z. U.; Jiang, H.-L. Metal-Organic Frameworks: Structures and Functional Applications. *Mater. Today* **2019**, *27*, 43–68.
6. Dhakshinamoorthy, A.; Li, Z.; Garcia, H. Catalysis and Photocatalysis by Metal Organic Frameworks. *Chem. Soc. Rev.* **2018**, *47*, 8134–8172.
7. Xiao, J.-D.; Jiang, H.-L. Metal-Organic Frameworks for Photocatalysis and Photothermal Catalysis. *Acc. Chem. Res.* **2019**, *52*, 356–366.
8. Liu, J.; Chen, L.; Cui, H.; Zhang, J.; Zhang, L.; Su, C.-Y. Applications of Metal-Organic Frameworks in Heterogeneous Supramolecular Catalysis. *Chem. Soc. Rev.* **2014**, *43*, 6011–6061.
9. Liu, D.; Wan, J.; Pang, G.; Tang, Z. Hollow Metal-Organic-Framework Micro/Nanostructures and Their Derivatives: Emerging Multifunctional Materials. *Adv. Mater.* **2019**, *31*, 1803291.
10. Huang, Y.-B.; Liang, J.; Wang, X.-S.; Cao, R. Multifunctional Metal-Organic Framework Catalysts: Synergistic Catalysis and Tandem Reactions. *Chem. Soc. Rev.* **2017**, *46*, 126–157.
11. Gong, W.; Liu, Y.; Li, H.; Cui, Y. Metal-Organic Frameworks as Solid Brønsted Acid Catalysts for Advanced

Organic Transformations. *Coord. Chem. Rev.* **2020**, *420*, 213400.
12. He, H.; Perman, J. A.; Zhu, G.; Ma, S. Metal–Organic Frameworks for CO_2 Chemical Transformations. *Small* **2016**, *12*, 6309–6324.
13. Ding, M.; Flaig, R. W.; Jiang, H.-L.; Yaghi, O. M. Carbon Capture and Conversion Using Metal-Organic Frameworks and MOF-Based Materials. *Chem. Soc. Rev.* **2019**, *48*, 2783–2828.
14. Zhou, D.-D.; Zhang, X.-W.; Mo, Z.-W.; Xu, Y.-Z.; Tian, X.-Y.; Li, Y.; Chen, X.-M.; Zhang, J.-P. Adsorptive Separation of Carbon Dioxide: From Conventional Porous Materials to Metal-Organic Frameworks. *EnergyChem* **2019**, *1*, 100016.
15. Zhang, T.; Jin, Y.; Shi, Y.; Li, M.; Li, J.; Duan, C. Modulating Photoelectronic Performance of Metal-Organic Frameworks for Premium Photocatalysis. *Coord. Chem. Rev.* **2019**, *380*, 201–229.
16. Xu, C.; Fang, R.; Luque, R.; Chen, L.; Li, Y. Functional Metal-Organic Frameworks for Catalytic Applications. *Coord. Chem. Rev.* **2019**, *388*, 268–292.
17. Shen, Y.; Pan, T.; Wu, P.; Huang, J.; Li, H.; Khalil, I. E.; Li, S.; Zheng, B.; Wu, J.; Wang, Q.; Zhang, W.; Wei, W. D.; Huo, F. Regulating Electronic Status of Pt Nanoparticles by Metal-Organic Frameworks for Selective Catalysis. *CCS Chem.* **2020**, *2*, 1607–1614.
18. Cui, W.-G.; Zhang, G.-Y.; Hu, T.-L.; Bu, X.-H. Metal-Organic Framework-Based Heterogeneous Catalysts for the Conversion of C_1 Chemistry: CO, CO_2 and CH_4. *Coord. Chem. Rev.* **2019**, *387*, 79–120.
19. Wang, C.; An, B.; Lin, W. Metal-Organic Frameworks in Solid-Gas Phase Catalysis. *ACS Catal.* **2019**, *9*, 130–146.
20. Zhu, L.; Liu, X.-Q.; Jiang, H.-L.; Sun, L.-B. Metal-Organic Frameworks for Heterogeneous Basic Catalysis. *Chem. Rev.* **2017**, *117*, 8129–8176.
21. Wu, Y.-P.; Tian, J.-W.; Liu, S.; Li, B.; Zhao, J.; Ma, L.-F.; Li, D.-S.; Lan, Y.-Q.; Bu, X. Bi-Microporous Metal-Organic Frameworks with Cubane $[M_4(OH)_4]$ (M=Ni, Co) Clusters and Pore-Space Partition for Electrocatalytic Methanol Oxidation Reaction. *Angew. Chem. Int. Ed.* **2019**, *58*, 12185–12189.
22. Lu, X. F.; Xia, B. Y.; Zang, S.-Q.; Lou, X. W. Metal-Organic Frameworks Based Electrocatalysts for the Oxygen Reduction Reaction. *Angew. Chem. Int. Ed.* **2020**, *59*, 4634–4650.
23. Chen, Y.-J.; Huang, X.; Chen, Y.; Wang, Y.-R.; Zhang, H.; Li, C.-X.; Zhang, L.; Zhu, H.; Yang, R.; Kan, Y.-H.; Li, S.-L.; Lan, Y.-Q. Polyoxometalate-Induced Efficient Recycling of Waste Polyester Plastics into Metal-Organic Frameworks. *CCS Chem.* **2019**, *1*, 561–270.
24. Hu, X.-J.; Li, Z.-X.; Xue, H.; Huang, X.; Cao, R.; Liu, T.-F. Designing a Bifunctional Brønsted Acid-Base Heterogeneous Catalyst through Precise Installation of Ligands on Metal-Organic Frameworks. *CCS Chem.* **2019**, *2*, 616–622.
25. Yuan, S.; Feng, L.; Wang, K.; Pang, J.; Bosch, M.; Lollar, C.; Sun, Y.; Qin, J.; Yang, X.; Zhang, P.; Wang, Q.; Zou, L.; Zhang, Y.; Zhang, L.; Fang, Y.; Li, J.; Zhou, H.-C. Stable Metal-Organic Frameworks: Design, Synthesis, and Applications. *Adv. Mater.* **2018**, *30*, 1704303.
26. Ding, M.; Cai, X.; Jiang, H.-L. Improving MOF Stability: Approaches and Applications. *Chem. Sci.* **2019**, *10*, 10209–10230.
27. Burtch, N. C.; Jasuja, H.; Walton, K. S. Water Stability and Adsorption in Metal-Organic Frameworks. *Chem. Rev.* **2014**, *114*, 10575–10612.
28. Bai, Y.; Dou, Y.; Xie, L.-H.; Rutledge, W.; Li, J.-R.; Zhou, H.-C. Zr-Based Metal-Organic Frameworks: Design, Synthesis, Structure, and Applications. *Chem. Soc. Rev.* **2016**, *45*, 2327–2367.
29. Howarth, A. J.; Liu, Y.; Li, P.; Li, Z.; Wang, T. C.; Hupp, J. T.; Farha, O. K. Chemical, Thermal and Mechanical Stabilities of Metal-Organic Frameworks. *Nat. Rev. Mater.* **2016**, *1*, 15018.
30. Yuan, S.; Qin, J.-S.; Lollar, C. T.; Zhou, H.-C. Stable Metal-Organic Frameworks with Group 4 Metals: Current Status and Trends. *ACS Cent. Sci.* **2018**, *4*, 440–450.
31. Qadir, N. u.; Said, S. A. M.; Bahaidarah, H. M. Structural Stability of Metal Organic Frameworks in Aqueous Media-Controlling Factors and Methods to Improve Hydrostability and Hydrothermal Cyclic Stability. *Microporous Mesoporous Mater.* **2015**, *201*, 61–90.
32. Li, N.; Xu, J.; Feng, R.; Hu, T.-L.; Bu, X.-H. Governing Metal-Organic Frameworks towards High Stability. *Chem. Commun.* **2016**, *52*, 8501–8513.
33. Zhao, X.; Yang, H.; Nguyen, E. T.; Padilla, J.; Chen, X.; Feng, P.; Bu, X. Enabling Homochirality and Hydrothermal Stability in Zn_4O-Based Porous Crystals. *J. Am. Chem. Soc.* **2018**, *140*, 13566–13569.
34. Xie, L.-H.; Xu, M.-M.; Liu, X.-M.; Zhao, M.-J.; Li, J.-R. Hydrophobic Metal-Organic Frameworks: Assessment, Construction, and Diverse Applications. *Adv. Sci.* **2020**, *7*, 1901758.
35. Jayaramulu, K.; Geyer, F.; Schneemann, A.; Kment, Š.; Otyepka, M.; Zboril, R.; Vollmer, D.; Fischer, R. A. Hydrophobic Metal-Organic Frameworks. *Adv. Mater.* **2019**, *31*, 1900820.
36. Mukherjee, S.; Sharma, S.; Ghosh, S. K. Hydrophobic Metal-Organic Frameworks: Potential toward Emerging Applications. *APL Mater.* **2019**, *7*, 050701.
37. Jiang, Z.-R.; Ge, J.; Zhou, Y.-X.; Wang, Z. U.; Chen, D.; Yu, S.-H.; Jiang, H.-L. Coating Sponge with a Hydrophobic Porous Coordination Polymer Containing a Low-Energy CF_3-Decorated Surface for Continuous Pumping Recovery of an Oil Spill from Water. *NPG Asia Mater.* **2016**, *8*, e253.
38. Zhang, W.; Hu, Y.; Ge, J.; Jiang, H.-L.; Yu, S.-H. A Facile and General Coating Approach to Moisture/Water-Resistant Metal-Organic Frameworks with Intact Porosity. *J. Am. Chem. Soc.* **2014**, *136*, 16978–16981.
39. Sun, Q.; He, H.; Gao, W.-Y.; Aguila, B.; Wojtas, L.; Dai, Z.; Li, J.; Chen, Y.-S.; Xiao, F.-S.; Ma, S. Imparting Amphiphobicity on Single-Crystalline Porous Materials. *Nat. Commun.* **2016**, *7*, 13300.
40. Sun, D.; Adiyala, P. R.; Yim, S.-J.; Kim, D.-P. Pore-Surface Engineering by Decorating Metal-Oxo Nodes with Phenylsilane to Give Versatile Super-Hydrophobic Metal-Organic Frameworks (MOFs). *Angew. Chem. Int. Ed.* **2019**, *58*, 7405–7409.

DOI: 10.31635/ccschem.020.202000515
CCS Chem. **2020**, *2*, 2740–2748

41. Liu, T.-F.; Zou, L.; Feng, D.; Chen, Y.-P.; Fordham, S.; Wang, X.; Liu, Y.; Zhou, H.-C. Stepwise Synthesis of Robust Metal-Organic Frameworks via Postsynthetic Metathesis and Oxidation of Metal Nodes in a Single-Crystal to Single-Crystal Transformation. *J. Am. Chem. Soc.* **2014**, *136*, 7813–7816.
42. Gamage, N.-D. H.; McDonald, K. A.; Matzger, A. J. MOF-5-Polystyrene: Direct Production from Monomer, Improved Hydrolytic Stability, and Unique Guest Adsorption. *Angew. Chem. Int. Ed.* **2016**, *55*, 12099–12103.
43. Ding, N.; Li, H.; Feng, X.; Wang, Q.; Wang, S.; Ma, L.; Zhou, J.; Wang, B. Partitioning MOF-5 into Confined and Hydrophobic Compartments for Carbon Capture Under Humid Conditions. *J. Am. Chem. Soc.* **2016**, *138*, 10100–10103.
44. Lian, X.; Feng, D.; Chen, Y.-P.; Liu, T.-F.; Wang, X.; Zhou, H.-C. The Preparation of an Ultrastable Mesoporous Cr(III)-MOF via Reductive Labilization. *Chem. Sci.* **2015**, *6*, 7044–7048.
45. Hou, L.; Wang, L.; Zhang, N.; Xie, Z.; Dong, D. Polymer Brushes on Metal-Organic Frameworks by UV-Induced Photopolymerization. *Polym. Chem.* **2016**, *7*, 5828–5834.
46. Qian, X.; Sun, F.; Sun, J.; Wu, H.; Xiao, F.; Wu, X.; Zhu, G. Imparting Surface Hydrophobicity to Metal-Organic Frameworks Using a Facile Solution-Immersion Process to Enhance Water Stability for CO_2 Capture. *Nanoscale* **2017**, *9*, 2003–2008.
47. Yang, S.; Peng, L.; Sun, D. T.; Asgari, M.; Oveisi, E.; Trukhina, O.; Bulut, S.; Jamali, A.; Queen, W. L. A New Post-Synthetic Polymerization Strategy Makes Metal-Organic Frameworks More Stable. *Chem. Sci.* **2019**, *10*, 4542–4549.
48. Carné-Sánchez, A.; Stylianou, K. C.; Carbonell, C.; Naderi, M.; Imaz, I.; Maspoch, D. Protecting Metal-Organic Framework Crystals from Hydrolytic Degradation by Spray-Dry Encapsulating Them into Polystyrene Microspheres. *Adv. Mater.* **2015**, *27*, 869–873.
49. Bao, S.; Li, J.; Guan, B.; Jia, M.; Terasaki, O.; Yu, J. A Green Selective Water-Etching Approach to MOF@Mesoporous SiO_2 Yolk-Shell Nanoreactors with Enhanced Catalytic Stabilities. *Matter* **2020**, *3*, 332–334.
50. Castells-Gil, J.; Novio, F.; Padial, N. M.; Tatay, S.; Ruíz-Molina, D.; Martí-Gastaldo, C. Surface Functionalization of Metal-Organic Framework Crystals with Catechol Coatings for Enhanced Moisture Tolerance. *ACS Appl. Mater. Interfaces* **2017**, *9*, 44641–44648.
51. He, S.; Wang, H.; Zhang, C.; Zhang, S.; Yu, Y.; Lee, Y.; Li, T. A Generalizable Method for the Construction of MOF@polymer Functional Composites through Surface-Initiated Atom Transfer Radical Polymerization. *Chem. Sci.* **2019**, *10*, 1816–1822.
52. Chui, S. S.-Y.; Lo, S. M.-F.; Charmant, J. P. H.; Orpen, A. G.; Williams, I. D. A Chemically Functionalizable Nanoporous Material $[Cu_3(TMA)_2(H_2O)_3]_n$. *Science* **1999**, *283*, 1148–1150.
53. Britt, D.; Tranchemontagne, D.; Yaghi, O. M. Metal-Organic Frameworks with High Capacity and Selectivity for Harmful Gases. *Proc. Natl. Acad. Sci. U. S. A.* **2008**, *105*, 11623–11627.
54. Karmakar, A.; Mileo, P. G. M.; Bok, I.; Peh, S. B.; Zhang, J.; Yuan, H.; Maurin, G.; Zhao, D. Thermo-Responsive MOF/Polymer Composites for Temperature-Mediated Water Capture and Release. *Angew. Chem. Int. Ed.* **2020**, *59*, 11003–11009.
55. Beyazit, S.; Bui, B. T. S.; Haupt, K.; Gonzato, C. Molecularly Imprinted Polymer Nanomaterials and Nanocomposites by Controlled/Living Radical Polymerization. *Prog. Polym. Sci.* **2016**, *62*, 1–21.
56. Chen, M.; Zhong, M.; Johnson, J. A. Light-Controlled Radical Polymerization: Mechanisms, Methods, and Applications. *Chem. Rev.* **2016**, *116*, 10167–10211.
57. Nesvadba, P. Radical Polymerization in Industry. In *Encyclopedia of Radicals in Chemistry, Biology and Materials*; John Wiley & Sons: Chichester, United Kingdom, **2012**, 1–36.
58. Haruvy, Y.; Gilath, I.; Maniewictz, M.; Eisenberg, N. Sol-Gel Replication of Microoptical Elements and Arrays. *Chem. Mater.* **1997**, *9*, 2604–2615.
59. Dizman, B.; Elasri, M. O.; Mathias, L. J. Synthesis, Characterization, and Antibacterial Activities of Novel Methacrylate Polymers Containing Norfloxacin. *Biomacromolecules* **2005**, *6*, 514–520.
60. Isoda, K.; Kuroda, K. Interlamellar Grafting of γ-Methacryloxypropylsilyl Groups on Magadiite and Copolymerization with Methyl Methacrylate. *Chem. Mater.* **2000**, *12*, 1702–1707.
61. Mazaj, M.; Čendak, T.; Buscarino, G.; Todaro, M.; Zabukovec Logar, N. Confined Crystallization of a HKUST-1 Metal-Organic Framework within Mesostructured Silica with Enhanced Structural Resistance towards Water. *J. Mater. Chem. A* **2017**, *5*, 22305–22315.
62. Banerjee, R.; Phan, A.; Wang, B.; Knobler, C.; Furukawa, H.; O'Keeffe, M.; Yaghi, O. M. High-Throughput Synthesis of Zeolitic Imidazolate Frameworks and Application to CO_2 Capture. *Science* **2008**, *319*, 939–943.
63. Dan-Hardi, M.; Serre, C.; Frot, T.; Rozes, L.; Maurin, G.; Sanchez, C.; Férey, G. A New Photoactive Crystalline Highly Porous Titanium(IV) Dicarboxylate. *J. Am. Chem. Soc.* **2009**, *131*, 10857–10859.
64. Wang, C.; Liu, X.; Demir, N. K.; Chen, J. P.; Li, K. Applications of Water Stable Metal-Organic Frameworks. *Chem. Soc. Rev.* **2016**, *45*, 5107–5134.
65. Kitanosono, T.; Masuda, K.; Xu, P.; Kobayashi, S. Catalytic Organic Reactions in Water toward Sustainable Society. *Chem. Rev.* **2018**, *118*, 679–746.
66. Kaur, N.; Kaur, S.; Kaur, G.; Bhalla, A.; Srinivasan, S.; Chaudhary, G. R. Metallovesicles as Smart Nanoreactors for Green Catalytic Synthesis of Benzimidazole Derivatives in Water. *J. Mater. Chem. A* **2019**, *7*, 17306–17314.
67. Yang, Q.; Xu, Q.; Jiang, H.-L. Metal-Organic Frameworks Meet Metal Nanoparticles: Synergistic Effect for Enhanced Catalysis. *Chem. Soc. Rev.* **2017**, *46*, 4774–4808.

DOI: 10.31635/ccschem.020.202000515
CCS Chem. **2020**, *2*, 2740–2748